

## Infrared Color-Sorting Metasurface: Supplementary Information

GUANGHAO CHEN<sup>1+</sup>, JUNXIAO ZHOU<sup>1+</sup>, LI CHEN<sup>2</sup>, FANGLIN TIAN<sup>1</sup>, ZHAOWEI LIU<sup>1,2\*</sup>

<sup>1</sup>Department of Electrical and Computer Engineering, University of California, San Diego, 9500 Gilman Drive, La Jolla, California 92093, United States

<sup>2</sup>Department of Materials Science and Engineering, University of California, San Diego, La Jolla, California 92093, United States

\* [zhaowei@ucsd.edu](mailto:zhaowei@ucsd.edu)

<sup>+</sup>These authors contributed equally to this work.

### NOTE A: GROUP DELAY OF A GRATING

With the designated angles of the input and output channels, the angular dispersion can be calculated with the grating equation,  $Gm\lambda = \sin \theta_i + \sin \theta_t$ , in which  $G$  is the magnitude of the grating reciprocal vector  $\vec{G}$  and  $\lambda$  is the incident wavelength.  $\theta_i$  and  $\theta_t$  correspond to the incident and diffraction angles, respectively [1]. In this design, the energy is diffracted into the 1<sup>st</sup> diffraction order ( $m = 1$ ). When expressed in terms of frequency, the diffraction angle of the beam is given by:

$$\theta_t = \text{asin} \left[ \frac{2\pi c_0 G}{\omega} - \sin \theta_i \right] \quad (\text{A1})$$

where  $c_0$  is the speed of light in vacuum. In the case of narrow bandwidth, the angular dispersion is calculated as:

$$\frac{d\theta_t}{d\omega} = \frac{2\pi c_0 G}{\omega^2 \sqrt{1 - \left( \frac{2\pi c_0 G}{\omega} - \sin \theta_i \right)^2}} = \frac{1}{\omega} \left[ \frac{\sin(\theta_i)}{\cos(\theta_t)} + \tan(\theta_t) \right] \approx \frac{1}{\omega_0} \left[ \frac{\sin(\theta_i)}{\cos(\theta_t)} + \right] \quad (\text{A2})$$

The angular dispersion is linear to the frequency. The phase delay in reference to the central frequency  $\omega_0$  is:

$$\phi(x; \omega) = -\frac{\omega x}{c_0} \sin \left[ \theta_t + \frac{d\theta_t}{d\omega} (\omega - \omega_0) \right] \quad (\text{A3})$$

The GD  $\phi'$  of the grating is given by:

$$\phi'(x; \omega) = \frac{\partial \phi(x; \omega)}{\partial \omega} \Big|_{\omega = \omega_0} = -\frac{x}{c_0} \sin \left[ \theta_t + \frac{d\theta_t}{d\omega} (\omega - \omega_0) \right] \quad (\text{A4})$$

At narrowband condition, the GD  $\phi'(x; \omega)$  can be approximated as  $-x/c_0 \sin(\theta_t)$ , which is a linear function of  $x$ .

### NOTE B: GROUP DELAY OF A PAIR OF HUYGENS' RESONATORS

In a dielectric particle, the electrical dipole (ED,  $e$ ) and magnetic dipole (MD,  $m$ ) resonances are the dominant modes, when the size of the particle is small compared to the incident

wavelengths. When approximated by Lorentzian line shapes [2], the forward scattering efficiency can be expressed as

$$t(\omega) = 1 + \frac{2i\gamma_e\omega}{\omega_e^2 - \omega^2 - 2i\gamma_e\omega} + \frac{2i\gamma_m\omega}{\omega_m^2 - \omega^2 - 2i\gamma_m\omega} \quad (\text{B1})$$

Here,  $\gamma_{e,m}$  is the damping factor and  $\omega_{e,m}$  denotes the resonance frequency. A Huygens' resonator is made when the first Kerker's condition [3], i.e.,  $\omega_e \approx \omega_m \approx \omega_0$  and  $\gamma_e \approx \gamma_m \approx \gamma$ , is met in a particle, such that both the transmission and the dispersion are maximized simultaneously at the resonant frequency. The phase is given by:

$$\phi = \arctan \left[ -\frac{4\gamma\omega(\omega_0^2 - \omega^2)}{(\omega_0^2 - \omega^2)^2 - 4\gamma^2\omega^2} \right] \quad (\text{B2})$$

To observe the dispersion near the resonance more clearly, we express the parameters in Eq. (B2) in terms  $\omega_0$ , i.e.,  $\gamma = \gamma'\omega_0$  and  $\omega = \omega_0 + x\omega_0$ . Hence, the GD and the GDD are, respectively,

$$\phi'(x, \gamma') = -\frac{4\gamma'(2 + x(2 + x))}{4\gamma'^2(1 + x)^2 + x^2(2 + x)^2} \quad (\text{B3})$$

$$\phi''(x, \gamma') = \frac{8\gamma'(1 + x)(4\gamma'^2 + x(2 + x)(4 + x(2 + x)))}{(4\gamma'^2(1 + x)^2 + x^2(2 + x)^2)^2} \quad (\text{B4})$$

where  $\partial\phi/\partial x = \omega_0\partial\phi/\partial\omega$  and  $\partial^2\phi/\partial x^2 = \omega_0^2\partial^2\phi/\partial\omega^2$ . In the wavelength range used in this work,  $\delta\omega \approx 0.55\omega_0$  and  $\gamma'$  is estimated at 0.1 by fitting the simulated transmittance. Both functions are plotted in Fig. 2 (a) and (b). A small GDD can only be found at large damping where dispersion is small. In the existence of another Huygens' resonance, the accumulated GD is given by:

$$\begin{aligned} \phi'(\omega; \gamma_1, \gamma_2, \omega_1, \omega_2) &= \phi'(\omega; \gamma_1, \omega_1) + \phi'(\omega; \gamma_2, \omega_2) \\ &= -\frac{4\gamma_1(\omega_1^2 - \omega^2)}{\omega_1^4 + 4\gamma_1^2\omega^2 - 2\omega_1^2\omega^2 + \omega^4} - \frac{4\gamma_2(\omega_2^2 - \omega^2)}{\omega_2^4 + 4\gamma_2^2\omega^2 - 2\omega_2^2\omega^2 + \omega^4} \end{aligned} \quad (\text{B5})$$

Again, we can express the parameters in terms of  $\omega_0$ , i.e.,  $\gamma_1 = g_1\omega_0$ ,  $\gamma_2 = g_2\omega_0$ ,  $\omega_1 = \omega_0 - \delta\omega_0/2$ ,  $\omega_2 = \omega_0 + \delta\omega_0/2$ , and  $\omega = \omega_0 + x\omega_0$ , where  $\delta$  tunes the frequency offsets of both resonances. Eq. (B5) can be rewritten as:

$$\begin{aligned} \phi'(x; \delta, q_1, q_2) &= \phi'(\omega; \gamma_1, \omega_1) + \phi'(\omega; \gamma_2, \omega_2) \\ &= -\frac{16\gamma_2(8 + \delta(4 + \delta) + 4x(2 + x))}{8\delta^3 + \delta^4 - 32\delta x(2 + x) - 8\delta^2(-2 + x(2 + x)) + 16(4\gamma_2^2(1 + x) \dots)} \end{aligned} \quad (\text{B6})$$

Similarly, the scaled GDD is the derivative of  $\phi'(x; \delta, q_1, q_2)$  with respect to  $x$ . The GDs and GDDs are plotted in Fig. 2 (c) and (d).

### NOTE C: METASURFACE SIMULATION

In the design, four layers of Huygens' resonators are stacked inside a metasurface, with each layer is associated with a resonance wavelength at one of the four band edges. The metasurface unit cells in the design are made of silicon ( $n = 3.41$ ) nanodisks embedded in a  $\text{CaF}_2$  ( $n = 1.23$ ) substrate, as shown in Fig. 5 (a). Periodic boundary conditions are applied at the four sides of the unit cell and perfectly matched layers are applied on the top and the bottom of the cell.

After roughly determining the size of the particles, the diameter ( $D$ ), height ( $H$ ) and unit cell width ( $P$ ) in each layer are further optimized in the wave optics module of COMSOL to shift the resonances to the desired wavelengths. Afterwards,  $H$  and  $P$  are set to constant for each layer, leaving  $D$  as the only parameter to detune the resonances.

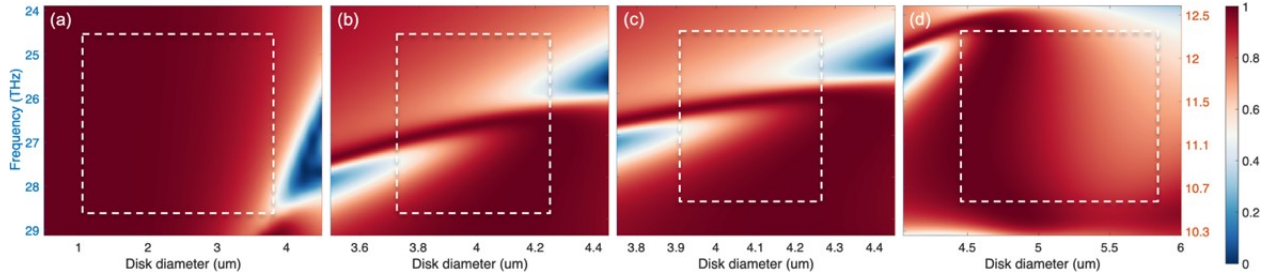


Fig. S1. Transmittance of the four selected groups of resonances: (a) 10.4  $\mu\text{m}$ , (b) 11.2  $\mu\text{m}$ , (c) 11.43  $\mu\text{m}$ , and (d) 12.3  $\mu\text{m}$ . The blue vertical axis on the left indicates the frequency and the red vertical axis is the corresponding wavelength in  $\mu\text{m}$ . The white dashed boxes mark the high transmittance regions ( $T > 70\%$ ) that are used in our design.

### NOTE D: WAVELENGTH-SPLITTING DEVICE OPTIMIZATION

The purpose of device optimization is to find out the best meta-atom size combinations that yield good device performance. Oblique incident plane waves pass through the grating and the metasurface with mostly phase modulated. The far-field radiation pattern is then simulated via scalar diffraction with the Fraunhofer approximation. Ideally, a full-wave simulation should be implemented in the optimization loop for best accuracy, but the excessive computation will be prohibitive. There are over 100 meta-atoms in the metasurface and each meta-atom is associated with two parameters, as shown in Fig. 4. Therefore, in this demonstration, we only use full-wave simulation to compute the complex transmission coefficients of the meta-atoms at several resonance conditions, i.e., combinations of  $H$  and  $P$ . The optimization then selects from this library of pre-computed meta-atoms.

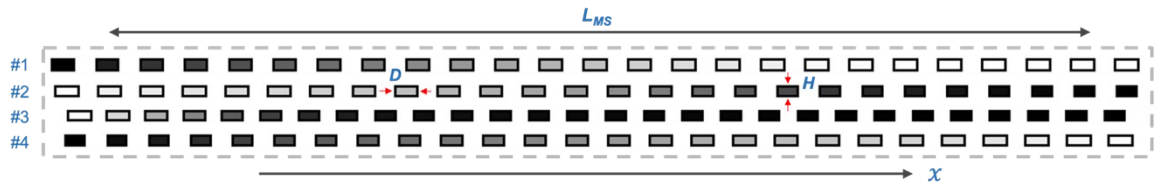


Fig. S2. Cross section of the optimized metasurface with 4 layers of meta-atoms. The diameters of the meta-atoms are varied along the  $X$  direction. From the top layer #1 to the bottom layer #4, the resonance wavelengths of meta-atoms at each layer are tuned around 12.3  $\mu\text{m}$ , 11.43  $\mu\text{m}$ , 11.2  $\mu\text{m}$ , and 10.4  $\mu\text{m}$ , respectively. The total length of the simulated region,  $L_{MS}$ , is 210  $\mu\text{m}$ .

In the simulation, the metasurface is considered a stack of four thin phase elements with a gap of 4  $\mu\text{m}$  between adjacent layers, shown in Fig. S2. Each phase element consists of an array of detuned meta-atoms varied in the diameters. The complex transmission coefficient of each meta-atom is interpolated from the maps shown in Fig. 6. In the setting of the simulation domain, each layer of the metasurface has roughly 25 meta-atoms and more than 100 units in

total. The optimization is carried out on a home-built Python program with TensorFlow [4]. It combines the built-in automatic differentiation tool and a stochastic gradient descent (SGD) optimizer to drive the metasurface design. After each iteration, the broadband far-field radiation pattern is evaluated by a merit function that promotes angular separation of the two bands and minimizes angular dispersion in each band. The centroid of each band, as shown in Fig.5 (c) and (f), is computed as the intensity-weighted average of the angles and the broadband angular dispersion is measured by computing the standard deviation of angles at all computed wavelengths. Based on the result, the SGD algorithm ends each iteration by adjusting the design parameters in the direction of maximal cost reduction.

## References

1. C. Palmer, and E. G. Loewen, (2005).
2. M. Decker, I. Staude, M. Falkner, J. Dominguez, D. N. Neshev, I. Brener, T. Pertsch, and Y. S. Kivshar, *Adv. Opt. Mater.* **3**, 813-820 (2015).
3. W. Liu, and Y. S. Kivshar, *Opt. Express* **26**, 13085-13105 (2018).
4. M. Abadi, P. Barham, J. Chen, Z. Chen, A. Davis, J. Dean, M. Devin, S. Ghemawat, G. Irving, and M. Isard, "Tensorflow: A system for large-scale machine learning," in *12th USENIX symposium on operating systems design and implementation (OSDI 16)*(2016), pp. 265-283.